



Characterization of Strength and Quality of Cemented Mine Backfill Made up of Lead-Zinc Processing Tailings

Ufuk Gokhan Akkaya^{1*}, Kenan Cinku¹ and Erol Yilmaz²

¹Department of Mining Engineering, Faculty of Engineering, Istanbul University-Cerrahpasa, Istanbul, Turkey, ²Department of Civil Engineering, Geotechnical Division, Recep Tayyip Erdogan University, Rize, Turkey

OPEN ACCESS

Edited by:

Antonio Caggiano,
Darmstadt University of Technology,
Germany

Reviewed by:

Mamadou Fall,
University of Ottawa, Canada
Jie Xin,
Institute of Rock and Soil Mechanics
(CAS), China
Wei-Ting Lin,
National Ilan University, Taiwan

*Correspondence:

Ufuk Gokhan Akkaya
ufukhan@iuc.edu.tr

Specialty section:

This article was submitted to
Structural Materials,
a section of the journal
Frontiers in Materials

Received: 12 July 2021

Accepted: 27 August 2021

Published: 14 September 2021

Citation:

Akkaya UG, Cinku K and Yilmaz E
(2021) Characterization of Strength
and Quality of Cemented Mine Backfill
Made up of Lead-Zinc
Processing Tailings.
Front. Mater. 8:740116.
doi: 10.3389/fmats.2021.740116

Predicting the reactions of the backfill materials exposed to the effects of air and groundwater will eventually ensure an efficient and accurate mine fill system for sustainable mining operations. This paper reveals the effect of the mobility of sulfur ions within lead-zinc processing tailings on strength and quality of cemented mine backfills. Some laboratory tests such as X-ray diffraction, ion chromatography, scanning electron microscopy, combustion tests, chemical analysis, pH and zeta potential measurements were performed to better characterize the backfill's mechanical and microstructural properties. Moreover, CEM II/A-P Portland pozzolan and CEM IV/A pozzolanic cements as ready-to-use cement products were used for cemented mine backfill preparation. To ensure the carrier of the lead-zinc tailings and to prevent the mobility of the sulfurous components, a binder content ranging from 3 to 7 wt % were employed in mine backfills. The experimental findings demonstrate that the used cement type and proportions were insufficient and some fractures are occurred in the samples due to the sulfur ion mobility. Accordingly, one can state clearly that the elemental analysis through the combustion test method can provide fast and reliable results in the determination of sulfur within lead-zinc processing tailings.

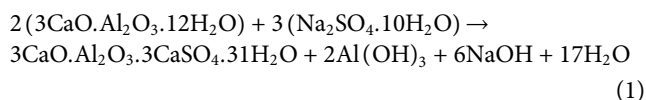
Keywords: sulphurous tailing, sulphate attack, mine backfill, hydraulic binder, mechanical strength

INTRODUCTION

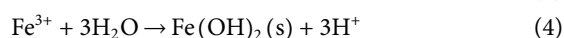
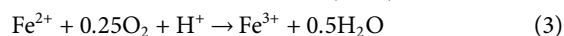
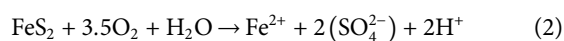
Environmentally sensible mining requires finding different solutions for mineral processing tailings (Qi and Fourie, 2019). Conventional methods such as tailings impoundments are not safe, and they are insufficient to store large amounts of the generated tailings by conservative environmental regulations (Chen et al., 2019; Cao et al., 2021). However, a huge amount of processing tailings can be stored in large gaps or by using filling techniques environmentally friendly (Jiang et al., 2020; Liu et al., 2020). Cemented paste backfill (CPB) is a commonly-employed technique, especially in Canada, China and Australia, in which underground openings called stopes are supported by being filled with high voluminous tailings (Lu et al., 2018; Cao et al., 2021). In addition, ensuring the harmlessness and environmental compatibility of the processing tailings, the durability plays a key role on the overall performance of CPB samples (Libos and Cui, 2020). Typically, CPB is prepared in a surface paste plant by dewatering fine tailings to form a filter cake, then a sufficient amount of mixing water and binder agents is added to create the mixture pumpable to underground stopes (Kou et al., 2020). Since CPB offers several significant environmental, technical, and economic benefits, it is

considered as one of the best available techniques in Europe for the management of tailings (Chen et al., 2021). However, the physical and chemical properties of CPB should be explored exactly before delivering a cost-effective and high-performance backfill to mines (Yang et al., 2020; Cavusoglu et al., 2021). Hence, interactions between the adjacent environment and processing tailings must be considered for surface/underground mining operations.

The tailings stored underground, especially in metal mining, can cause harmful ion mobility and acid mine drainage (AMD) when they interact with oxygen and underground and/or rain waters (Koohestani et al., 2020). The risk of AMD is related to the presence of sulfidic minerals such as pyrite (FeS_2) (Zhao, 2021). The presence of sulfides within cemented composites has a deleterious effect on paste backfill strength due to sulfate attack (Koohestani et al., 2021). Sulfate attack plays a main role in the mechanical strength and service life of concrete (Liu et al., 2020). However, the mechanisms of sulfate attack on CPB are not quite similar to those on concrete. The sulfate attack on CPB is internal, whereas that on concrete is predominantly external. Moreover, in CPB, sulfate can be adsorbed on the surface of C-S-H, thereby weakening the strength of CPB, since C-S-H is largely responsible for the strength development of any cementitious material (Wang et al., 2020; Alainachi & Fall 2020; Koohestani et al., 2018). Conventional sulfate attack in mortar and concrete leads to the formation of expansive ettringite and gypsum (Eq. 1) (Jiang et al., 2020).



Ettringite minerals cause expanding during sulfate attack in concrete, leading cracking, spalling, and spillage (Baquerizo et al., 2016). The very low solubility of brucite shifts the above reaction to the right side and favors the consumption of calcium hydroxide (Park et al., 2019). This leads to a reduction in pH and, as a result, calcium silicate hydrate (C-S-H) becomes more susceptible to sulfate attack (Mafra et al., 2020). Sulfate attack is directly related to pH of the tailings and its surroundings (Belebchouche et al., 2016). CPB includes iron, silicon, and aluminum hydroxides as well as gypsum at pH values under 9 (Xiapeng et al., 2019). The risks of contaminated neutral drainage within rocks that contain carbonate compounds and AMD occur at moderate (6–8) and low (<5) pH values, respectively (Myagkaya et al., 2020). AMD is eventually formed by the oxidation of pyrite (Eqs 2, 3, 4).



Sulfide-bearing minerals can jeopardize paste structures by lowering pH and degrading the hydrate, resulting in rapid reactivity depending on the saturation and presence of O_2 (Nordstrom et al., 2015). The oxidation process plays an essential role in the conversion of ferrous iron to ferric iron.

Each pH value above 4 contributes to this process (Jiménez & Prieto, 2015). When pH is less than 4, AMD occurs through the contribution of iron-oxidizing ferrooxidant bacteria (Levio-Raiman et al., 2021). The bacterium *thiobacillus ferrooxidans* increases the initial acidification when the pH is above 4.5. Below pH 4.5, *thiobacillus ferrooxidans* allows acidification to continue by oxidizing Fe^{2+} from pyritic materials (Shirin et al., 2021). Compounds of calcium (CaCO_3 , $\text{CaMg}(\text{CO}_3)_2$), iron (FeCO_3 , $\text{Fe}(\text{OH})_3$), and magnesium (MgCO_3) are key factors for neutralizing AMD from mine tailings (Elghali et al., 2021). In near-neutral mine waters, along with SO_4^{2-} , bicarbonate (HCO_3^-) is a significant anion. In addition, the concentrations of dissolved calcium (Ca^{2+}) and magnesium (Mg^{2+}) ions are generally elevated relative to dissolved iron (Fe^{3+}) and aluminum (Al^{3+}), which precipitate as the pH increases to above 4–5. Hydrolysis reactions cause many metal ions to form the hydroxides with low solubility. Even dissolved gases can undergo hydration. The hydration reactions of dissolved carbon dioxide (CO_2) and sulfur dioxide (SO_2) form carbonic acid (H_2CO_3) and sulfuric acid (H_2SO_3), respectively (Othmani et al., 2015).

Tricalcium aluminate (C_3A) and tetra calcium aluminoferrite (C_4AF) are the most critical compounds to be considered in sulfate-rich processing tailings (Zheng et al., 2017). According to the ASTM C150-07 standard, the C_3A content should not exceed 5% in sulfate resisting cement, while the combined $\text{C}_3\text{A} + \text{C}_4\text{AF}$ amount should be much lower than 25%. Both Portland and Portland-based cements have great importance in the immobilization and storage of hazardous wastes (Zheng et al., 2018). Ettringite is an important structure for immobilizing contaminants. While the creation of ettringite at early stages is linked with the use of added sulfates to avoid flash sets, its formation at later stages due to external sulfate attack or delayed ettringite formation can cause degradation of concrete structures (Gu et al., 2019). In mine backfill applications, the cement is often used to prevent the AMD formation, and also to offer the mechanical strength, which is critical for the stability of CPB (Hefni and Ali, 2021). To reduce/eliminate the negative effects of AMD which is harmful to vegetation, aquatic life, wildlife, groundwater, and strength of mine backfill (Li et al., 2020; Wang et al., 2021), many researchers have studied to reduce the amount of the cement needed by using different types of cement and additives (Xue et al., 2020; Yan et al., 2020; Huan et al., 2021).

This paper presents an experimental investigation of sulfide-bearing tailings and their possibility of utilization in CPB with two different cement types (CEM II and CEM IV) and amounts (3 and 7 wt%). The originality of this research paper lies in addressing the study of ion chromatography and combustion test conducted on CPB samples containing sulfide-rich minerals. To reveal the interaction with sulfurous compounds such as SO_3 and SO_4 , the zeta potential values in CPB were also measured.

MATERIALS AND METHODS

Characterization of Lead-Zinc Processing Tailings

In this study, sulfide-rich tailings sampled from a lead-zinc mineral processing plant in Turkey were employed for the preparation of CPB samples. Several analyses on X-ray

TABLE 1 | Chemical analysis of binders types used during the experiments.

| Compounds | CEM II/A-P Portland Pozzolan | CEM IV/A Pozzolan |
|--|------------------------------|-------------------------|
| SiO ₂ (%) | 17.84 | 30.82 |
| Al ₂ O ₃ (%) | 4.32 | 6.53 |
| Fe ₂ O ₃ (%) | 2.99 | 4.00 |
| CaO (%) | 61.64 | 49.64 |
| MgO (%) | 2.06 | 2.01 |
| SO ₃ (%) | 2.93 | 2.33 |
| Cl (%) | 0.01 | 0.04 |
| Na ₂ O/K ₂ O (%) | — | 0.68/0.93 |
| CaO-free lime (%) | 1.68 | 0.70 |
| Insoluble residue (%) | 0.78 | 14.13 |
| Undefined (%) | 2.45 | 0.10 |
| Loss of ignition (%) | 5.76 | 2.92 |
| Mineralogical composition (%) | — | 7.58 (C ₃ A) |

diffraction (XRD), inductively coupled plasma mass spectrometry (ICP-MS) and ion chromatography were performed for determining the mineralogical and chemical composition of dry and wet tailings samples. To authenticate the state of the mineral phases visually, scanning electron microscopy (SEM) analyses were done. Since the particle size distribution may affect greatly the dissolution rate of the tailings, the particle size distribution analysis was also conducted according to the TS 1,500 standard (equivalent to the ASTM D2487 standard) using the Malvern MS3000 particle size analyzer which measures particles from 10 nm up to 3.5 mm.

Characterization of Binder and Mixing Water

pH measurements were done to reveal interactions between CPB and its storage environment (with the groundwater adjacent rocks and soils). Indeed, the zeta potential of particles is an important indicator of the interaction between them at different pH values (Jiang et al., 2020; Xu et al., 2021). An increase in the zeta potential increases the water retention ability of pastes that are prepared in the particulate environment. The Zeta potential measurements of each dry paste backfill materials were made by concerning pH using a Brookhaven NanoBrook Zeta Plus zeta potential analyzer.

In order to investigate the interaction between the tailings material (1 wt%) and its surroundings, the change in the pH of the medium was determined with respect to time in pH profile experiments. In these experiments, the HCl and NaOH solutions were used to adjust the ambient pH (2, 3, 5.7, 10, and 11).

In this study, two types of Portland Pozzolan (CEM II/A-P) and Pozzolan (CEM IV/A) type cement produced by Akcansa Co. (Turkey) were used as hydraulic binders. Note that both of them are suitable to employ in cementitious works conducted in aggressive areas where the sulfate and chloride ions are relatively high. The specifications of these two cement types are presented in **Table 1**.

Preparation of Mine Backfills

After the characterization tests, the unconfined compressive strength (UCS) tests were conducted for determining the

mechanical behavior of CPB materials containing two types of different commercial and ready-to-use cement products (CEM II and CEM IV). For the UCS tests, 36 cylindrical samples were prepared in a length/diameter ratio of 2/1. These were formed with every 3 samples from both types of cement (CEM II and CEM IV), at two cement ratios (3 and 7 wt%), and three different curing times (7, 14, and 28 days). The slump values ranging from 6 to 10 inches (15.24–25.40 cm) were used for the pumpability of the CPB material in a pipeline. The CPB slump recipes are given in **Table 2**.

Chemical and Microstructural Measurements

The elemental analysis by combustion (LECO 628 S), ion chromatography tests (ICS 1100), and SEM analysis (Jeol JSM 5600) was performed for investigating sulfide-rich compounds, ion release, and their effects on ettringite occurrence. To determine the amount of sulfur in ettringite, the elemental analysis by combustion and ion chromatography was carried out. Meanwhile, to determine the total sulfur in concrete that causes the SO₃ and SO₄ movement, the combustion tests was carried out.

RESULTS AND DISCUSSION

Particle Size Distribution, XRD, Conductivity, pH and Zeta Potential Results of Tailings

From the particle size distribution tests, the tailings were found to have 42 wt% particles finer than 20 μm, classifying the tailings as medium size grained particles which seem to have lower strengths. It also provides the relatively high specific surface of the grains to ensure sufficient surface tension which enables the solids to hold water and offer a thin permanent lubricating film creating the paste. Note that the grain size distribution of the tailings was classified as a homogeneous distribution according to the TS EN ISO14688-2 standard. The specific gravity of the tailings measured by using a helium pycnometer was found to have 3.2.

TABLE 2 | A summary of slump recipes of cemented mine backfills.

| Cement type | Amount of solids + cement + water (g) | Cement content (3 wt%) | Cement content (7 wt%) |
|------------------------------|---------------------------------------|------------------------|------------------------|
| CEM II/A-P Portland puzzolan | Solids | 10,000 | 10,000 |
| | Cement | 300 | 700 |
| | Water | 2,850 | 2,650 |
| | Slump value (cm) | 18.8 | 18.8 |
| CEM IV/A puzzolan cement | Solids | 10,000 | 10,000 |
| | Cement | 300 | 700 |
| | Water | 2,800 | 2,700 |
| | Slump value (cm) | 18.8 | 18.8 |

TABLE 3 | ICP MS results of the tailings.

| Oxides (%) | Base and precious metal elements (ppm) | | | | Rare earth elements (ppm) | | | | Radioactive elements (ppm) and others (%) | | | | |
|--------------------------------|--|----|-------|----|---------------------------|----|------|----|---|----|-----|-------|-------|
| SiO ₂ | 36.19 | Mo | 5.7 | Ba | 404 | La | 30.4 | Tm | 0.27 | Th | 9 | TOT/C | 3.16 |
| Al ₂ O ₃ | 8.08 | Cu | 217.2 | Co | 15.7 | Ce | 57.2 | Yb | 1.58 | U | 6.4 | TOT/S | 7.49 |
| Fe ₂ O ₃ | 13.58 | Pb | 1,500 | Rb | 76.4 | Pr | 6 | Lu | 0.23 | | | LOI | 12.4 |
| MgO | 2.54 | Zn | 1,548 | Sn | 11 | Nd | 20.9 | Yb | 17.2 | | | Sum | 99.48 |
| CaO | 23.26 | Ni | 29.4 | Sr | 191.3 | Sm | 3.86 | Sc | 7 | | | | |
| Na ₂ O | 0.2 | As | 601.8 | V | 62 | Eu | 0.99 | | | | | | |
| K ₂ O | 2.45 | Cd | 8.2 | W | 44.6 | Gd | 3.37 | | | | | | |
| TiO ₂ | 0.29 | Sb | 23.6 | Zr | 76.8 | Tb | 0.54 | | | | | | |
| P ₂ O ₅ | 0.08 | Bi | 26.5 | Hg | 0.37 | Dy | 2.87 | | | | | | |
| MnO | 0.38 | Ag | 3.7 | | | Ho | 0.55 | | | | | | |
| Cr ₂ O ₃ | 0.01 | Au | 0.055 | | | Er | 1.62 | | | | | | |

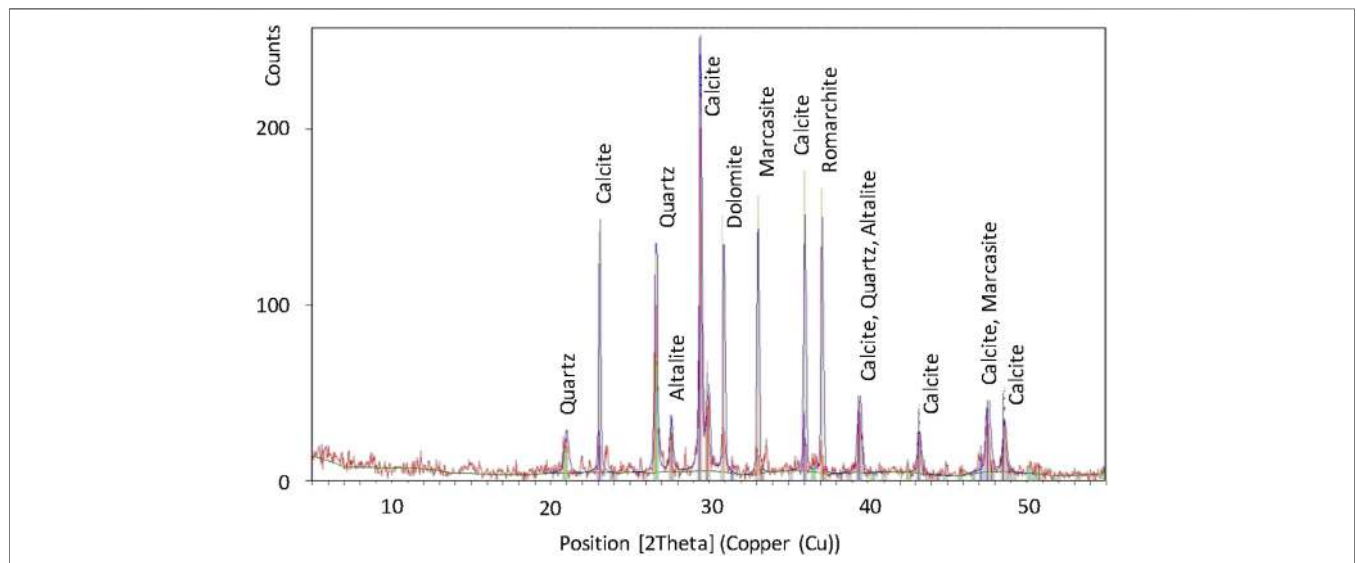


FIGURE 1 | XRD profile result of the tailings sample.

Table 3 lists the results of the ICP-MS analysis in the solids and process water of the tailings materials. Samples includes relatively high quantities of CaO, Fe₂O₃, Zn, Pb, and K. The XRD results (Figure 1) are the good agreement with these findings. In addition, the sulfurous contents were high in both dry materials

and tailings water according to the ICP-MS test. Earlier studies have shown that a chemical reaction occurs in the presence of sulfate and acid production and that as a consequence, the mechanical strength of the backfill material decreases (Hamberg et al., 2017; Cao et al., 2019; Li et al., 2019).

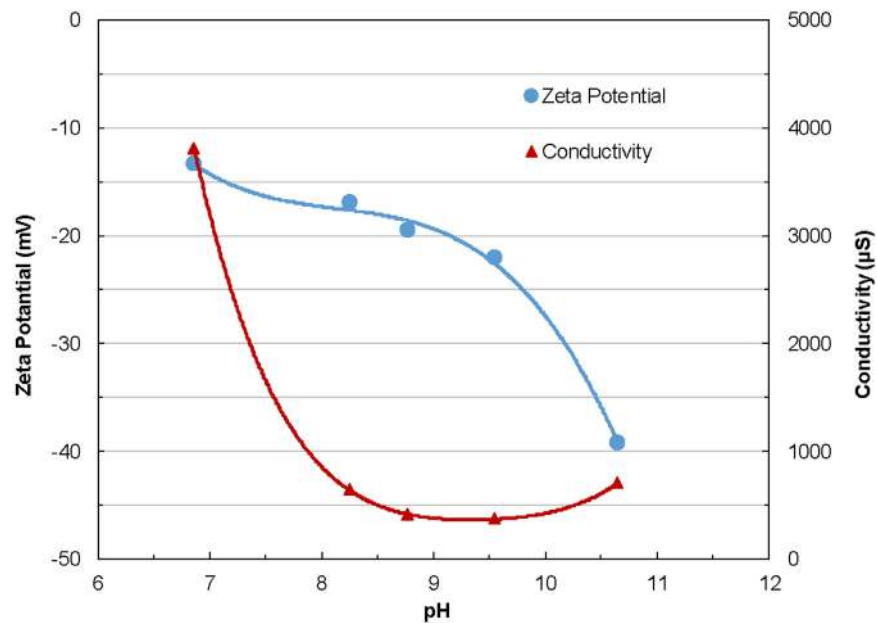


FIGURE 2 | Conductivity and the zeta potential profile of the tailings sample.

Consequently, it can be expected that the sulfate ions affect the cement applications negatively.

The binding of water molecules to fine particles at high zeta potential values provides high retention of paste backfill in a slump. The dry paste's zeta potential was negative. The negative character of dry paste was influenced by the relative abundance of Si^{4+} , Al^{3+} , Ca^{2+} , K^+ , and Mg^{2+} ions dissolved from the tailings. The zeta potential results of the tailings sample as a function of pH are given in **Figure 2**. It is clear from **Figure 2** that the zeta potential became more negative with the increasing pH. As the zeta potential of the particles becomes more negative with the increasing pH, the electrostatic repulsion forces increase.

Thus, the particles repel each other. OH^- ion increase resulting from the pH rise caused zeta potential increase negatively. This proves that OH^- is the potential determining ion and will assist in the uniform distribution of particles in the CPB matrix. This refers that the tailings are electro-kinetically stable, and the particles will be easily dispersed in the tailings. These results clearly show that the zeta potential-pH relationship plays a critical role in the stability and homogeneous distribution of paste backfill.

Considering the favorable pH range (pH 6–9) in the relevant regulation (Turkish Official Gazette: No. 25687) to discharge, it can be stated that the tested tailings-based material is in the stable zone (above 25 mV) at pH values above 9. The increase in the pH of the material with the addition of cement contributes to the backfill's stability in the stable zone, and therefore to the homogeneous distribution of the particles in the paste backfill matrix. In addition, the zeta potential results can be utilized to identify the type of anionic or cationic chemicals present for further studies. There are two main reasons why the conductivity (**Figure 2**) values were high at low pH levels. First, high

concentrations of NaOH were used to increase the pH of the medium and the second reason is the excessive Ca^{2+} , K^+ , and Mg^{2+} ions. It can also infer from the zeta potential and conductivity results (**Figure 2**) that since pH became more negative with increasing pH, OH^- ions are the potential determining ions.

The pH profile results are seen in **Figure 3**. As seen in **Figure 3**, buffering tended to bring the environmental pH to around 8.5–9 within the first 10 min. It was observed that this tendency occurs faster in the acidic medium and more slowly in the basic medium. Consequently, one can understand that the material possesses a buffering feature and tended to remain stable in this range. This means that the tailings will remain within the allowable pH limits (pH 6–9) of the wastewater discharge range for the mining industry specified in the regulations (Turkish Official Gazette No: 25,687), even when exposed to the effects of rainwater and groundwater. It can be inferred from the zeta potential and pH profile results that ion movement occurs in the material. The use of lime to suppress the acidity of the tailings is one of the reasons for the excessive Ca^{2+} and OH^- ions.

UCS Test Results of Cemented Backfill Samples

Figure 4 indicates the results of the UCS test results. It is clear that the UCS test samples became brittle and dispersions occurred as a result of the decreased cement content (3 wt%). The maximum UCS values (700 kPa) were obtained with 7 wt% CEMIV cement ratio at 28 curing days while the UCS values are varying between 0.05 and 4.35 MPa in previous studies (Jiang et al., 2020; Liu et al., 2020). Besides, the lowest UCS values (250 kPa after 28 days) were obtained with 3 wt% CEM IV cement. The results showed

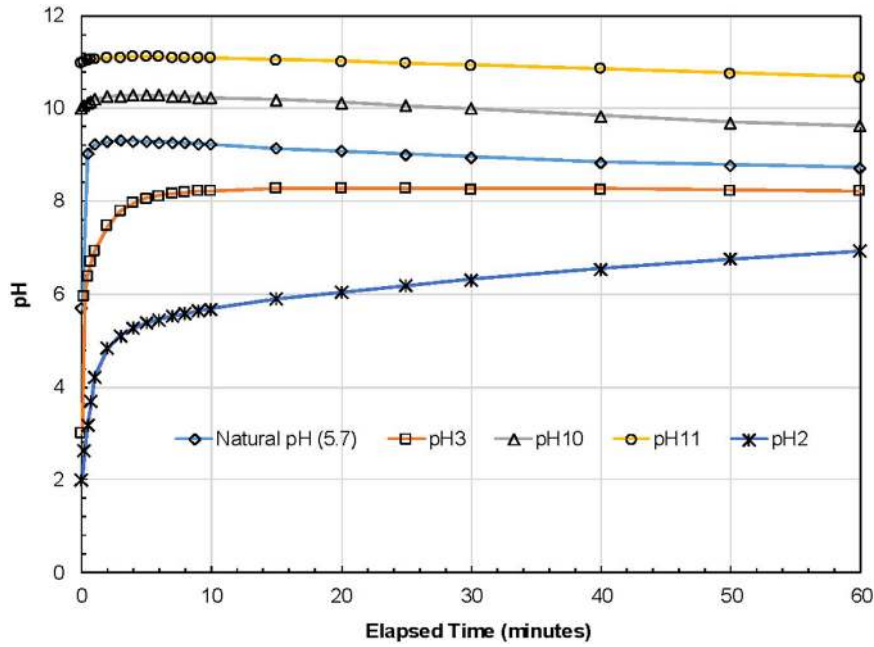


FIGURE 3 | pH profile results for the tested mine tailings.

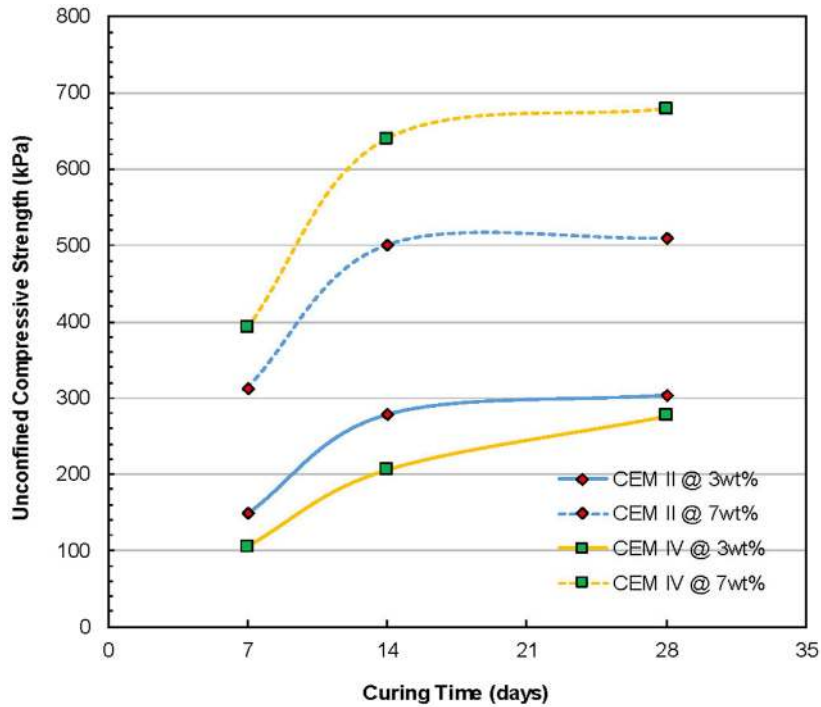


FIGURE 4 | UCS test results of different CPB samples as a function of curing time.

that there was no major difference between OPC and blended cement in the sulfur-rich CPB, in line with the reference (Li & Fall 2016).

The elemental analysis by combustion, ion chromatography, and SEM were performed to investigate the sulfurous compounds, ion release, and their effects on ettringite

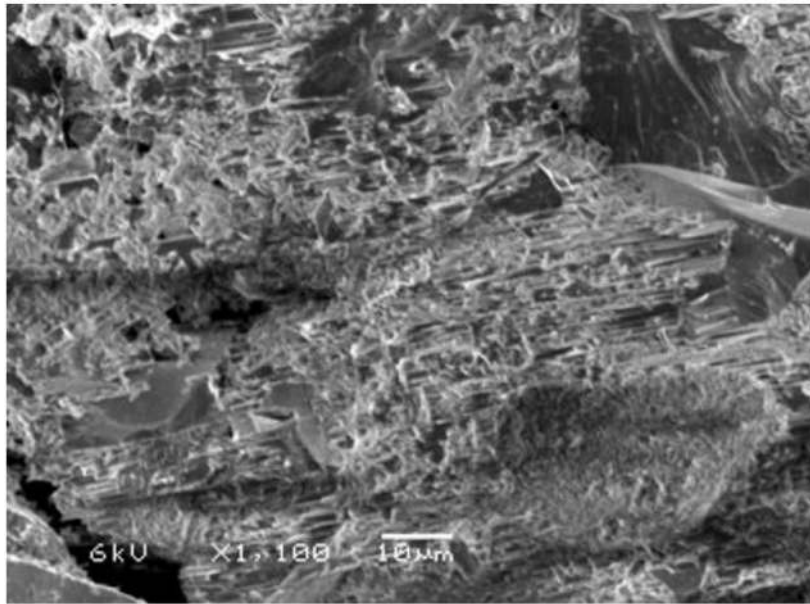


FIGURE 5 | The SEM micrograph of the tested CPB sample.

occurrence. The elemental analysis by combustion and ion chromatography were carried out to define the amount of sulfur in the ettringite. Meanwhile, the use of combustion tests was investigated to determine the total sulfur in the concrete that causes the SO_3 and SO_4 movement. It is important to identify the combustion temperature is vital to obtaining the maximum sulfur ratio. Jiménez and Prieto (Jiménez & Prieto, 2015) investigated the dehydration of ettringite in natural and synthetic samples and showed that the total weight loss in the thermo-gravimetric analysis at $1,000^\circ\text{C}$ was 45.5 and 40.5% for natural and synthetic samples, respectively. It was also stated that for synthetic samples, total weight losses of 32.6 and 35.6% were obtained at the temperatures of $190\text{--}300$ and $650\text{--}800^\circ\text{C}$, respectively due to the decomposition of calcite at calcination temperature. Moreover, the temperatures of 300 , 600 , 800 , $1,000$, and $1,350^\circ\text{C}$ were tested with 0.5 and 1.0 g samples. As a result, it was observed that the backfill sample melted at $1,350^\circ\text{C}$, and the highest sulfur amount was achieved at $1,000^\circ\text{C}$ with an amount of 0.5 g.

Analysis of Relationship Between UCS and Total Sulfur by Combustion Tests and SEM

Figure 5 demonstrates the SEM micrograph of CPB samples. Meanwhile, the results of the elemental analysis by combustion tests in Figure 6 and the ion analysis in Figure 7 indicated that the reason for the low UCS values (<1 MPa); It is due to sulfur ion mobility over the formation of ettringite within the cemented tailings. These consequences are compatible with the findings of Wang et al. (Wang et al., 2020).

It is clear from Figure 6 that the expected benefit from cement is realized as the curing time of concrete in two cement types and

at different rates increases. The amount of sulfur in CPB samples decreased and the corresponding mechanical strength increased. The fact that the CaO content in CEM II cement type is higher than CEM IV cement type suggests that secondary gypsum ($\text{CaSO}_4 \cdot 2\text{H}_2\text{O}$) minerals may occur more within the cemented backfills.

Analysis of Relationship Between UCS and Sulfate by Ion Analysis

When the results of the total sulfur and sulfate tests are compared, it can be seen that increasing the cement content from 3 to 7 wt% diminished the total sulfur amounts due to the residual stiffness. Similarly, the sulfate dispersion in the concrete was reduced due to the stiff structure when the cement amount was increased. The relationship between the obtained results and UCS is given in Figure 7.

It is apparent from Figure 7 that 3 wt% CPB samples containing CEM IV cement type provides the low mechanical strengths. This is mainly due to the high amount of Al in this cement at high sulfate content and the high formation of ettringite ($3\text{CaSO}_4 \cdot 3\text{CaO} \cdot \text{Al}_2\text{O}_3 \cdot 32\text{H}_2\text{O}$) with high expansion potential. In high cement quantities, as the curing time increases, the mobility of sulfate within the CPB sample and its conversion to ettringite will slow down.

Analysis of Time-dependent Sulfate and Sulfur Concentrates

Figure 8 demonstrates the relationship of the change in the sulfur and sulfate contents of CPB samples as a function of curing time. It is clear from Figure 8 that sulfur tends to decrease continuously due to the effect of added cement and slaked lime within CPB samples. On the other hand, the sulfate content tends to increase

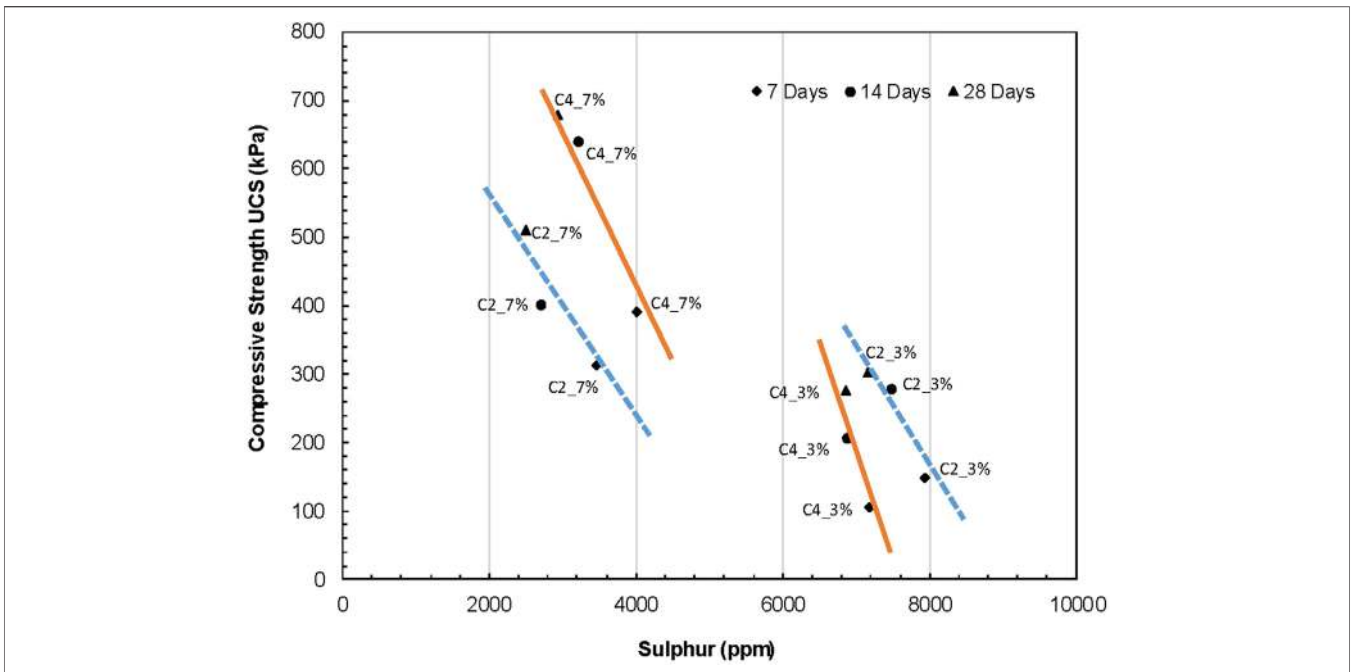


FIGURE 6 | The relationship between the UCS and total sulfur results (by combustion).

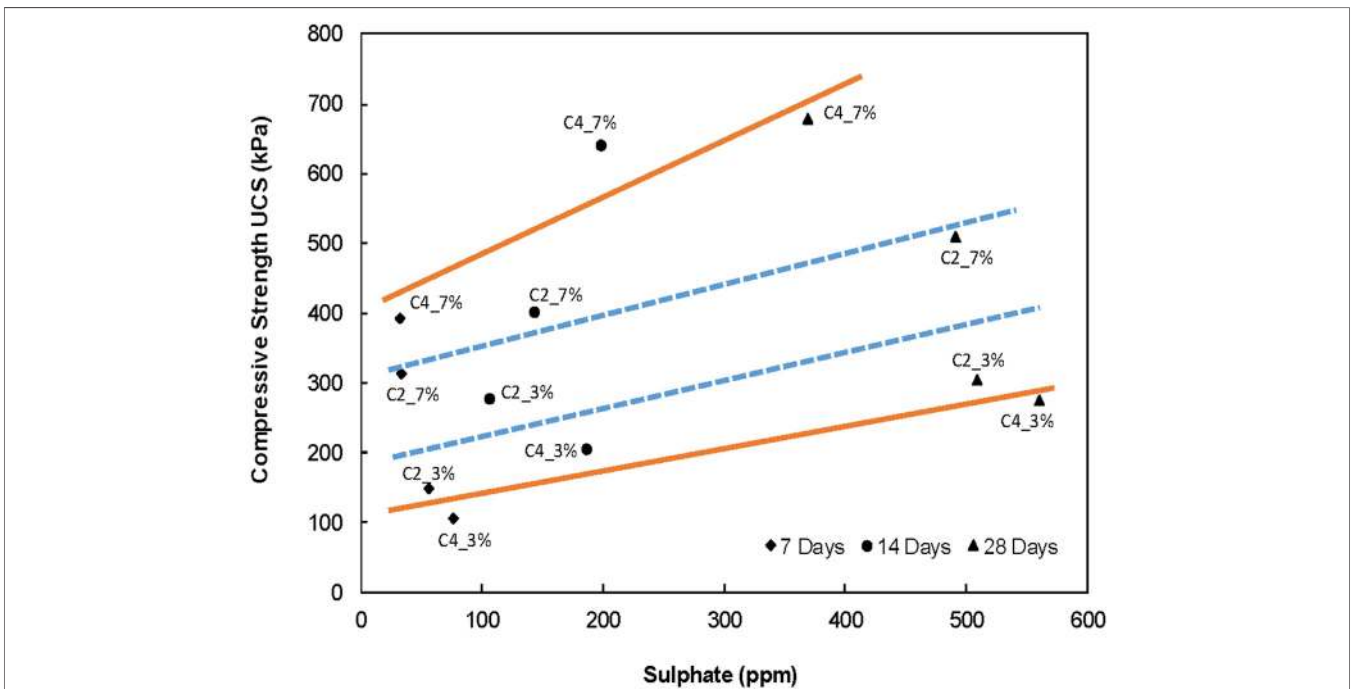


FIGURE 7 | The relationship between UCS and sulfate results (by ion analysis).

continuously, especially from the 7th day. Both findings are compatible with Li et al. (Li et al., 2019).

In the cementitious matrices subjected to sulfate attack, the amount of sulfate ions decreases as the reaction and curing time continues and thus the rate of sulfate attack is inclined to

decelerate. The mineral phases (ettringite and gypsum) resulting from the reactions of sulfates with hydration products play a vital role on strength and quality of CPB samples (Gu et al., 2019). The formation of ettringite could generate expansive pressure that tangibly harms CPB samples.

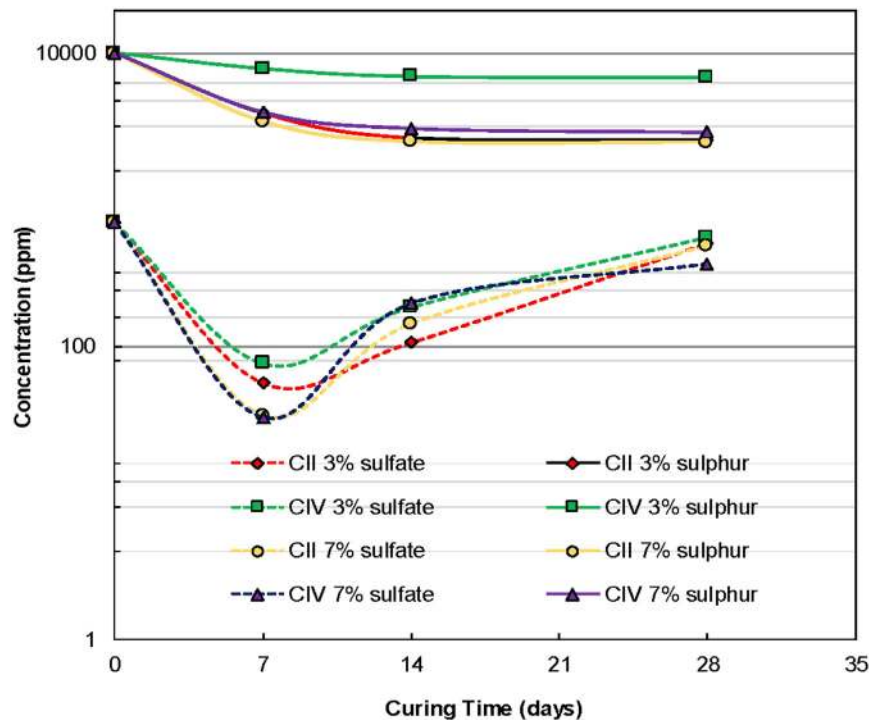


FIGURE 8 | Time-dependent sulfate (by ion analysis) and sulfur (by combustion) concentrations.

In the presence of sulfates, calcium hydroxide created during the cement hydration can lead to the making of gypsum (a source of strength degradation) in CPB.

CONCLUSION

In this study, the usability of Pb-Zn processing tailings in the paste backfill form was investigated experimentally. Several laboratory experiments such as unconfined compressive strength, particle size distribution, pH measurements, elemental analysis by combustion, ion chromatography, SEM, and the zeta potential were undertaken on CPB samples. From the performed experimental tests, the following main findings could be drawn:

- ✓ Although the tailings were mixed with blended cement, the mechanical strengths of paste backfill were relatively low due to expansive components and internal sulfate attack.
- ✓ The gypsum problem also occurred in the samples, as discovered by the SEM analysis.
- ✓ As the amount of sulfur within the paste backfill material decreased and the sulfate contents and mechanical strengths increased.
- ✓ The CEM IV type cement with a dosage of 7 wt% yielded higher UCS values than the CEM II type cement with a dosage of 3 wt%.
- ✓ From the SEM images, one can conclude that the increase in the sulfate content was due to the formation of ettringite, which caused the strengths to remain at relatively low values.

As a result of this study, it is suggested that the combustion test will give fast and accurate results for future CPB applications. In today's CPB applications, especially in high sulfur mines, it is predicted that the use of cement at high dosages (greater than a cement dosage of 7 wt%) and fast setting time can prevent the formation of secondary gypsum mineral and ettringite.

DATA AVAILABILITY STATEMENT

The raw data supporting the conclusion of this article will be made available by the authors, without undue reservation.

AUTHOR CONTRIBUTIONS

UA and KC conceived and designed the experiments and samples; UA prepared samples and performed the tests; UA, KC, and EY analyzed the data, UA and KC wrote the manuscript, UA and EY revised the manuscript. All authors read and approved the final manuscript.

FUNDING

This research was supported by The Scientific Research Projects Coordination Unit of Istanbul University-Cerrahpasa (Grant number: 40,888). Special acknowledgements are extended to Prof. Dr. Nuray Tokgoz for her precious contributions.

REFERENCES

- Alainachi, I., and Fall, M. (2020). Chemically Induced Changes in the Geotechnical Response of Cementing Paste Backfill in Shaking Table Test. *J. Rock Mech. Geotechnical Eng.* 13 (3), 513–528. doi:10.1016/j.jrmge.2020.11.002
- Baquerizo, L. G., Matschei, T., and Scrivener, K. L. (2016). Impact of Water Activity on the Stability of Ettringite. *Cement Concrete Res.* 79, 31–44. doi:10.1016/j.cemconres.2015.07.008
- Belebchouche, C., Moussaceb, K., and Ait-Mokhtar, A. (2016). Evaluation of the Encapsulation of Nickel, Chromium and Lead-Rich Wastes in Cement Matrices by TCLP Test. *Eur. J. Environ. Civil Eng.* 20 (7), 711–724. doi:10.1080/19648189.2015.1061458
- Cao, S., Xue, G., Yilmaz, E., and Yin, Z. (2021). Assessment of Rheological and Sedimentation Characteristics of Fresh Cemented Tailings Backfill Slurry. *Int. J. Mining, Reclamation Environ.* 35, 319–335. doi:10.1080/17480930.2020.1826092
- Cao, S., Xue, G., Yilmaz, E., Yin, Z., and Yang, F. (2021). Utilizing Concrete Pillars as an Environmental Mining Practice in Underground Mines. *J. Clean. Prod.* 278, 123433. doi:10.1016/j.jclepro.2020.123433
- Cao, S., Yilmaz, E., Song, W., and Xue, G. (2019). Assessment of Acoustic Emission and Triaxial Mechanical Properties of Rock-Cemented Tailings Matrix Composites. *Adv. Mater. Sci. Eng.* 2019, 1–12. doi:10.1155/2019/6742392
- Cavusoglu, I., Yilmaz, E., and Yilmaz, A. O. (2021). Additivity Effect on Properties of Cemented Coal Fly Ash Backfill Containing Water-Reducing Admixtures. *Construction Building Mater.* 267, 121021. doi:10.1016/j.conbuildmat.2020.121021
- Chen, Q., Tao, Y., Feng, Y., Zhang, Q., and Liu, Y. (2021). Utilization of Modified Copper Slag Activated by Na₂SO₄ and CaO for Unclassified Lead/Zinc Mine Tailings Based Cemented Paste Backfill. *J. Environ. Manage.* 290, 112608. doi:10.1016/j.jenvman.2021.112608
- Chen, X., Shi, X., Zhou, J., Du, X., Chen, Q., and Qiu, X. (2019). Effect of Overflow Tailings Properties on Cemented Paste Backfill. *J. Environ. Manage.* 235, 133–144. doi:10.1016/j.jenvman.2019.01.040
- Elghali, A., Benzaazoua, M., Bouzazhah, H., Abdelmoula, M., Dynes, J. J., and Jamieson, H. E. (2021). Role of Secondary Minerals in the Acid Generating Potential of Weathered Mine Tailings: Crystal-Chemistry Characterization and Closed Mine Site Management Involvement. *Sci. Total Environ.* 784, 147105. doi:10.1016/j.scitotenv.2021.147105
- Gu, Y., Martin, R.-P., Omikrine Metalssi, O., Fen-Chong, T., and Dangla, P. (2019). Pore Size Analyses of Cement Paste Exposed to External Sulfate Attack and Delayed Ettringite Formation. *Cement Concrete Res.* 123, 105766. doi:10.1016/j.cemconres.2019.05.011
- Hamberg, R., Maurice, C., and Alakangas, L. (2017). Lowering the Water Saturation Level in Cemented Paste Backfill Mixtures - Effect on the Release of Arsenic. *Minerals Eng.* 112, 84–91. doi:10.1016/j.mineng.2017.05.005
- Hefni, M., and Ali, M. A. (2021). The Potential to Replace Cement with Nano-Calcium Carbonate and Natural Pozzolans in Cemented Mine Backfill. *Adv. Civil Eng.* 2021, 1–10. doi:10.1155/2021/5574761
- Huan, C., Zhu, C., Liu, L., Wang, M., Zhao, Y., Zhang, B., et al. (2021). Pore Structure Characteristics and its Effect on Mechanical Performance of Cemented Paste Backfill. *Front. Mater.* 8, 700917. doi:10.3389/fmats.2021.700917
- Jiang, D., Li, X., Jiang, W., Li, C., Lv, Y., and Zhou, Y. (2020). Effect of Tricalcium Aluminate and Sodium Aluminate on Thaumate Formation in Cement Paste. *Construction Building Mater.* 259, 119842. doi:10.1016/j.conbuildmat.2020.119842
- Jiang, H., Fall, M., Yilmaz, E., Li, Y., and Yang, L. (2020). Effect of Mineral Admixtures on Flow Properties of Fresh Cemented Paste Backfill: Assessment of Time Dependency and Thixotropy. *Powder Technol.* 372, 258–266. doi:10.1016/j.powtec.2020.06.009
- Jiang, H., Han, J., Li, Y., Yilmaz, E., Sun, Q., and Liu, J. (2020). Relationship between Ultrasonic Pulse Velocity and Uniaxial Compressive Strength for Cemented Paste Backfill with Alkali-Activated Slag. *Nondestructive Test. Eval.* 35 (4), 359–377. doi:10.1080/10589759.2019.1679140
- Jiménez, A., and Prieto, M. (2015). Thermal Stability of Ettringite Exposed to Atmosphere: Implications for the Uptake of Harmful Ions by Cement. *Environ. Sci. Technol.* 49 (13), 7957–7964. doi:10.1021/acs.est.5b00536
- Koohestani, B., Darban, A. K., Darezeshki, E., Mokhtari, P., Yilmaz, E., and Yilmaz, E. (2018). The Influence of Sodium and Sulfate Ions on Total Solidification and Encapsulation Potential of Iron-Rich Acid Mine Drainage in Silica Gel. *J. Environ. Chem. Eng.* 6 (2), 3520–3527. doi:10.1016/j.jece.2018.05.037
- Koohestani, B., Darban, A. K., Mokhtari, P., Darezeshki, E., Yilmaz, E., and Yilmaz, E. (2020). Influence of Hydrofluoric Acid Leaching and Roasting on Mineralogical Phase Transformation of Pyrite in Sulfidic Mine Tailings. *Minerals* 10 (6), 513. doi:10.3390/min10060513
- Koohestani, B., Mokhtari, P., Yilmaz, E., Mahdipour, F., and Darban, A. K. (2021). Geopolymerization Mechanism of Binder-free Mine Tailings by Sodium Silicate. *Construction Building Mater.* 268, 121217. doi:10.1016/j.conbuildmat.2020.121217
- Kou, Y., Jiang, H., Ren, L., Yilmaz, E., and Li, Y. (2020). Rheological Properties of Cemented Paste Backfill with Alkali-Activated Slag. *Minerals* 10 (3), 288. doi:10.3390/min10030288
- Levio-Raiman, M., Briceño, G., Schalchli, H., Bornhardt, C., and Diez, M. C. (2021). Alternative Treatment for Metal Ions Removal from Acid Mine Drainage Using an Organic Biomixture as a Low Cost Adsorbent. *Environ. Technol. Innovation* 24, 101853. doi:10.1016/j.eti.2021.101853
- Li, J., Yilmaz, E., and Cao, S. (2020). Influence of Solid Content, Cement/Tailings Ratio, and Curing Time on Rheology and Strength of Cemented Tailings Backfill. *Minerals* 10 (10), 922. doi:10.3390/min10100922
- Li, W., and Fall, M. (2016). Sulphate Effect on the Early Age Strength and Self-Desiccation of Cemented Paste Backfill. *Construction Building Mater.* 106, 296–304. doi:10.1016/j.conbuildmat.2015.12.124
- Li, Y., Min, X., Ke, Y., Fei, J., Liu, D., and Tang, C. (2019). Immobilization Potential and Immobilization Mechanism of Arsenic in Cemented Paste Backfill. *Minerals Eng.* 138, 101–107. doi:10.1016/j.mineng.2019.04.041
- Libos, I. L. S., and Cui, L. (2020). Effects of Curing Time, Cement Content, and Saturation State on Mode-I Fracture Toughness of Cemented Paste Backfill. *Eng. Fracture Mech.* 235, 107174. doi:10.1016/j.engfracmech.2020.107174
- Liu, L., Xin, J., Huan, C., Qi, C., Zhou, W., and Song, K.-I. (2020). Pore and Strength Characteristics of Cemented Paste Backfill Using Sulphide Tailings: Effect of Sulphur Content. *Construction Building Mater.* 237, 117452. doi:10.1016/j.conbuildmat.2019.117452
- Liu, L., Xin, J., Qi, C., Jia, H., and Song, K.-I. (2020). Experimental Investigation of Mechanical, Hydration, Microstructure and Electrical Properties of Cemented Paste Backfill. *Construction Building Mater.* 263, 120137. doi:10.1016/j.conbuildmat.2020.120137
- Lu, H., Qi, C., Chen, Q., Gan, D., Xue, Z., and Hu, Y. (2018). A New Procedure for Recycling Waste Tailings as Cemented Paste Backfill to Underground Stopes and Open Pits. *J. Clean. Prod.* 188, 601–612. doi:10.1016/j.jclepro.2018.04.041
- Mafra, C., Bouzazhah, H., Stamenov, L., and Gaydardzhiev, S. (2020). Insights on the Effect of Pyrite Liberation Degree upon the Acid Mine Drainage Potential of Sulfide Flotation Tailings. *Appl. Geochem.* 123, 104774. doi:10.1016/j.apgeochem.2020.104774
- Myagkaya, I. N., Lazareva, E. V., Zaikovskii, V. I., and Zhmodik, S. M. (2020). Interaction of Natural Organic Matter with Acid Mine Drainage: Authigenic Mineralization (Case Study of Ursk Sulfide Tailings, Kemerovo Region, Russia). *J. Geochemical Exploration* 211, 106456. doi:10.1016/j.gexplo.2019.106456
- Nordstrom, D. K., Blowes, D. W., and Ptacek, C. J. (2015). Hydrogeochemistry and Microbiology of Mine Drainage: An Update. *Appl. Geochem.* 57, 3–16. doi:10.1016/j.apgeochem.2015.02.008
- Othmani, M. A., Souissi, F., Bouzazhah, H., Bussiére, B., da Silva, E. F., and Benzaazoua, M. (2015). The Flotation Tailings of the Former Pb-Zn Mine of Touiref (NW Tunisia): Mineralogy, Mine Drainage Prediction, Base-Metal Speciation Assessment and Geochemical Modeling. *Environ. Sci. Pollut. Res.* 22, 2877–2890. doi:10.1007/s11356-014-3569-1
- Park, I., Tabelin, C. B., Jeon, S., Li, X., Seno, K., Ito, M., et al. (2019). A Review of Recent Strategies for Acid Mine Drainage Prevention and Mine Tailings Recycling. *Chemosphere* 219, 588–606. doi:10.1016/j.chemosphere.2018.11.053
- Qi, C., and Fourie, A. (2019). Cemented Paste Backfill for Mineral Tailings Management: Review and Future Perspectives. *Minerals Eng.* 144, 106025. doi:10.1016/j.mineng.2019.106025
- Shirin, S., Jamal, A., Emmanouil, C., and Yadav, A. K. (2021). Assessment of Characteristics of Acid Mine Drainage Treated with Fly Ash. *Appl. Sci.* 11, 3910. doi:10.3390/app11093910

- Wang, S., Song, X., Wei, M., Liu, W., Wang, X. X., Ke, Y., et al. (2021). Experimental Study on the Effect of Alkalized Rice Straw Content on Mechanical Properties of Cemented Tailings Backfill. *Front. Mater.* (Inpress). doi:10.3389/fmats.2021.727925
- Wang, Y., Cao, Y., Cui, L., Si, Z., and Wang, H. (2020). Effect of External Sulfate Attack on the Mechanical Behavior of Cemented Paste Backfill. *Construction Building Mater.* 263, 120968. doi:10.1016/j.conbuildmat.2020.120968
- Xiapeng, P., Fall, M., and Haruna, S. (2019). Sulphate Induced Changes of Rheological Properties of Cemented Paste Backfill. *Minerals Eng.* 141, 105849. doi:10.1016/j.mineng.2019.105849
- Xu, W., Chen, W., Tian, M., and Guo, L. (2021). Effect of Temperature on Time-dependent Rheological and Compressive Strength of Fresh Cemented Paste Backfill Containing Flocculants. *Construction Building Mater.* 267, 121038. doi:10.1016/j.conbuildmat.2020.121038
- Xue, G., Yilmaz, E., Song, W., and Cao, S. (2020). Fiber Length Effect on Strength Properties of Polypropylene Fiber Reinforced Cemented Tailings Backfill Specimens with Different Sizes. *Construction Building Mater.* 241, 118113. doi:10.1016/j.conbuildmat.2020.118113
- Yan, B., Zhu, W., Hou, C., Yilmaz, E., and Saadat, M. (2020). Characterization of Early Age Behavior of Cemented Paste Backfill through the Magnitude and Frequency Spectrum of Ultrasonic P-Wave. *Construction Building Mater.* 249, 118733. doi:10.1016/j.conbuildmat.2020.118733
- Yang, L., Xu, W., Yilmaz, E., Wang, Q., and Qiu, J. (2020). A Combined Experimental and Numerical Study on the Triaxial and Dynamic Compression Behavior of Cemented Tailings Backfill. *Eng. Structures* 219, 110957. doi:10.1016/j.engstruct.2020.110957
- Zhao, D. (2021). Reactive MgO-Modified Slag-Based Binders for Cemented Paste Backfill and Potential Heavy-Metal Leaching Behavior. *Construction Building Mater.* 298, 123894. doi:10.1016/j.conbuildmat.2021.123894
- Zheng, J., Guo, L., SunLi, X. W., Li, W., and Jia, Q. (2018). Study on the Strength Development of Cemented Backfill Body from Lead-Zinc Mine Tailings with Sulphide. *Adv. Mater. Sci. Eng.* 2018, 1–8. doi:10.1155/2018/7278014
- Zheng, J., Guo, L., and Zhao, Z. (2017). Effect of Calcined Hard Kaolin Dosage on the Strength Development of CPB of Fine Tailings with Sulphide. *Adv. Mater. Sci. Eng.* 2017, 1–7. doi:10.1155/2017/8631074

Conflict of Interest: The authors declare that the research was conducted in the absence of any commercial or financial relationships that could be construed as a potential conflict of interest.

Publisher's Note: All claims expressed in this article are solely those of the authors and do not necessarily represent those of their affiliated organizations, or those of the publisher, the editors and the reviewers. Any product that may be evaluated in this article, or claim that may be made by its manufacturer, is not guaranteed or endorsed by the publisher.

Copyright © 2021 Akkaya, Cinku and Yilmaz. This is an open-access article distributed under the terms of the Creative Commons Attribution License (CC BY). The use, distribution or reproduction in other forums is permitted, provided the original author(s) and the copyright owner(s) are credited and that the original publication in this journal is cited, in accordance with accepted academic practice. No use, distribution or reproduction is permitted which does not comply with these terms.